Spatiotemporal hotspots of potential microbial risk in shower systems

Ren, Anran; Yao, Mingchen; Zhang, Yue; Chen, Lihua; Li, Xiaoming; Yan, Wei; van der Meer, Walter; Rose, Joan; Liu, Gang

DOI
10.1016/j.watres.2025.124028

Publication date
2025

Document Version
Final published version

Published in
Water Research

Citation (APA)
Ren, A., Yao, M., Zhang, Y., Chen, L., Li, X., Yan, W., van der Meer, W., Rose, J., & Liu, G. (2025). Spatiotemporal hotspots of potential microbial risk in shower systems. *Water Research*, *284*, Article 124028. https://doi.org/10.1016/j.watres.2025.124028

Water Research 284 (2025) 124028

Contents lists available at ScienceDirect

Water Research

journal homepage: www.elsevier.com/locate/watres

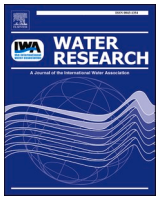

Spatiotemporal hotspots of potential microbial risk in shower systems

Anran Ren [a,b], Mingchen Yao [a,b], Yue Zhang [a,b], Lihua Chen [a,b], Xiaoming Li [a,b], Wei Yan [c], Walter van der Meer [d], Joan Rose [e], Gang Liu [a,b,f,*]

[a] Key Laboratory of Environmental Aquatic Chemistry, State Key Laboratory of Regional Environment and Sustainability, Research Centre for Eco-Environmental Sciences, Chinese Academy of Sciences, Beijing 100085, PR China
[b] University of Chinese Academy of Sciences, Beijing, PR China
[c] Changchun Yungu Technology Co., Ltd., Changchun, Jilin Province 100028, PR China
[d] Science and Technology, University of Twente, P.O. Box 217, 7500AE Enschede, The Netherlands
[e] Department of Fisheries and Wildlife, Michigan State University, East Lansing, MI 48823, USA
[f] Sanitary engineering, Department of Water management, Faculty of Civil Engineering and Geosciences, Delft University of Technology, P.O. Box 5048, 2600 GA Delft, The Netherlands

ARTICLE INFO

Keywords:
Shower system
Dynamic study
Hot spots
Legionella pneumophila
Mycobacterium spp

ABSTRACT

Shower systems create conditions conducive to the growth of opportunistic pathogens, but the timing and location of associated risks are poorly understood. In this study, we constructed 48 full size shower units with six incubation periods (4, 10, 16, 22, 30, and 40 weeks) and four water heater temperature (39, 45, 51, and 58 °C) to examine the dynamics of microbial growth and pathogen distribution. Results showed that during the initial stage (4 weeks), peak biomass was observed for all biofilms, ranked as shower hose (SHE) > cold-water pipe (CWP) > hot-water pipe (HWP), followed by a sharp decline by the 10th-week. At the 4th-week, the biofilm was loose and easily detached into the water, possibly promoted by leached organic carbon from plastic material, fostering the growth of specific microorganisms. The impacts of stagnation and temperature became more pronounced in CWP and HWP over time. *Legionella pneumophila* appeared in biofilms at the 4th-week, disappeared, and reappeared in large numbers since the 22nd-week. Differently, *Mycobacterium* spp. emerged in large numbers after 30 weeks. Both pathogens were notably enriched in showerheads and shower hoses. This study highlights critical periods of higher risk in shower systems, particularly in the early stages (4 weeks) and after 22 weeks, suggesting that risks can be mitigated by pre-soaking pipes or regularly cleaning (e.g., heat shock flushing) and replacing showerheads and hoses.

1. Introduction

Waterborne diseases are a significant public health concern, with widespread global attention (Kunz et al., 2024; Pouey et al., 2021; Samuelsson et al., 2023). In 2014, the United States reported 1.13 million cases of waterborne infections linked to drinking water, resulting in 47,700 hospitalizations, 3300 deaths, and $1.39 billion in direct healthcare costs (Gerdes et al., 2023). From 2015 to 2020, 87 % of outbreaks associated with drinking water were due to biofilm pathogens, such as *Legionella* spp. and nontuberculous mycobacteria (NTM) (Kunz et al., 2024). Shower systems, with long stagnation times, low residual chlorine levels, high surface-to-volume ratios, and abundant nutrients, promote biofilm growth and are hotspots for opportunistic pathogens (Cordes et al., 1981; Proctor et al., 2018; Shen et al., 2022; Whiley et al., 2015). For instance, *Legionella* spp. was found in 31 % of home shower samples in the UK (Collins et al., 2017), and 70 % of showerheads in the US contained NTM (Feazel et al., 2009). Aerosols containing these pathogens can cause respiratory infections when inhaled during showering, making shower systems a potential infection source (Schoen and Ashbolt, 2011; Shen et al., 2022; Whiley et al., 2015). Thus, understanding microbial dynamics in shower systems is crucial for managing microbiological risks.

Shower systems are complex, consisting of hot- and cold-water pipes, shower hoses, showerheads, shower valves, and other components. Most field studies focus on easily accessible components, like showerheads and hoses, while the hot and cold pipes remain underrepresented (Cordes et al., 1981; Feazel et al., 2009; Proctor et al., 2018; Soto-Giron et al., 2016). The impact of temperature on biofilms, particularly in hot

* Corresponding author at: Research Center for Eco-Environmental Sciences, Chinese Academy of Sciences, Beijing, PR China.
E-mail addresses: gliu@rcees.ac.cn, g.liu-1@tudelft.nl (G. Liu).

https://doi.org/10.1016/j.watres.2025.124028
Received 15 April 2025; Received in revised form 9 June 2025; Accepted 13 June 2025
Available online 14 June 2025

water systems, has received limited attention. In some simulation studies, water temperature in hot water systems was gradually increased by 2.5 to 7 °C every 5 to 12 weeks in the same simulated device (Proctor et al., 2017; Rhoads et al., 2015). However, the influence of temperature on biofilms under the same similar incubation times in hot water system is underexplored. Therefore, a comprehensive study on microbial and pathogen dynamics across all shower system stages is necessary to fully assess the risk profile.

Although biofilm dynamics in drinking water pipes have been studied, focusing on materials, hydraulic conditions, and biomass (Douterelo et al., 2018; Manuel et al., 2007; Martiny et al., 2003; Rochex et al., 2008), most research has concentrated on cold water pipes, with limited data on biofilms in warm- and hot-water systems. Showers often use plastic pipes (e.g., shower hoses), which release dissolved organic carbon (DOC) that promotes biofilm growth (Learbuch et al., 2021; Romera-Castillo et al., 2018). Pathogens prefer biofilm environments; for example, *Legionella* spp. correlates with the age of the house (Hayes-Phillips et al., 2019), and L. *pneumophila* colonizes later in biofilm development (Abu Khweek and Amer, 2018), while NTM readily attaches to pipe surfaces (Pereira et al., 2020). Despite studies examining the impacts of temperature, pipe material, disinfectant, and water age on pathogen colonization (Falkinham, 2011; Farhat et al., 2012; Moritz et al., 2010; Wang et al., 2012), the dynamics of opportunistic pathogen growth in biofilms remain poorly understood. Understanding these dynamics could help reduce the risk of shower infections by identifying temporal and spatial hot spots of potential risks, and more importantly, a better understanding of such dynamics allows for the identification of effective control measures.

To address these gaps, this study constructed 48 full size shower units with four water heater temperature settings (39, 45, 51, and 58 °C) and six incubation periods (4, 10, 16, 22, 30, and 40 weeks). While shorter-term studies (< 4 weeks) are indeed important, this investigation primarily focused on long-term biofilm development dynamics. The objective was to systematically explore the dynamics of biomass, diversity, community composition, and opportunistic pathogens over time in different components and phases of shower systems. The finding provides valuable insights into the health risks associated with shower systems, helping to inform consumers about when and where these risks may arise.

2. Materials and methods

2.1. Experimental setup and operation

Four identical full-scale shower systems were constructed in a laboratory in Changchun Jilin Province, China. Each system included an instantaneous water heater, one electric valve, one multifunctional online monitoring meter with two temperature probes and one flow probe, two switches, and thirteen identical shower units (Fig. S1). A shower unit consisted of a cold-water pipe (CWP), hot-water pipe (HWP), shower hose (SHE), showerhead (SHD), check valve, cold/hot-water switch, solenoid valves, and other components (Figs. S1 and S2). The CWP and HWP were made of ½-inch polypropylene random copolymer (PPR) pipes, with internal diameters of 1.61 cm and 1.48 cm, and lengths of approximately 1.1 m and 1.0 m, respectively. The SHE was made of polyvinyl chloride (PVC) with an internal diameter of 0.85 cm and a length of 1.45 m. The SHD had a diameter of 9.3 cm and featured 45 silicone holes (internal diameter 1 mm, rain type) and 6 acrylonitrile-butadiene-styrene (ABS) plastic holes (internal diameter 2 mm, massage type). In this study, rain-type and massage-type showerhead spray patterns were used. The check valves and switches were made of stainless steel. The four instantaneous water heaters were set to temperatures of 39, 45, 51, and 58 °C, respectively. Unless otherwise specified, temperature refers to the water heater setting.

The water supply for the shower system was provided by approximately 30 m of ¾-inch PPR pipe, connected to a service line in a neighboring community. The shower system operated for 40 weeks (W), from August 2022 to May 2023. Each shower unit was flushed three times per week, with each flush lasting 8 min at a flow rate of 4.2 ± 0.4 L/min and an outlet water temperature of 39 ± 2 °C. The backup shower unit (closest to the water heater) was flushed first for 8 min to purge stagnant water from the premise plumbing, delivering chlorinated fresh shower water. Subsequently, the remaining 12 units were flushed sequentially at 2-minute intervals. The same flushing procedure was repeated for the 13 shower units at each of the four different temperature settings, ensuring all temperatures were flushed. The shower units were flushed automatically by switching the solenoid valves on and off according to a pre-set program. During periods of stagnation, the shower systems were allowed to cool to room temperature (19.5 to 25 °C). When the water heater temperature is set at 39 °C, the hot water heated by the water heater flows through the hot-water pipe directly into the shower hose. During this process, no cold water is mixed into the shower hose, so the cold-water pipe remains stagnant for a long time until the next sample is taken when the cold-water pipe is replenished with fresh water. The 39 °C temperature setting simulates the thermostatic anti-scald safety mode recommended by shower suppliers.

We conducted a 7-day TOC leaching experiment with CWP, HWP, and SHE, which demonstrated that plastic pipes can leach TOC, particularly the shower hoses. Notably, the TOC leaching rates decreased with increasing incubation time. Experimental details and results are provided in the Supplementary Materials (Text S1 and Figure S3).

2.2. Water and biofilm sampling

Water and biofilm samples were taken from the duplicate shower units of four temperature settings (39, 45, 51, and 58 °C) at 4th, 10th, 16th, 22nd, 30th, and 40th week of incubation. For the water samples, the freshwater (FHW) samples were collected at the tap on the main inlet pipe after sterilizing the tap with 75 % alcohol. Following a 5-min flushing, 2.2 L of FHW was collected in a sterilized glass bottle. After stagnation of 48 h, stagnant water (SGW) was sampled. To ensure sufficient SGW sample originated from the pipe, 250 mL (39 °C) or 500 mL (45, 51, and 58 °C) were collected (Table S1). After flushing the shower for 5 min, 2.2 L of shower water (SHW) sample was collected. Both SHW and SGW samples were collected from the showerhead.

Before biofilm sampling, the pipe surfaces, and surrounding environment were disinfected with 75 % alcohol. For biofilm in showerheads (SHD), a sterile rayon swab (Copan, Brescia, Italy) was used to scrape all holes in the showerheads. For biofilm in shower hose (SHE), the shower hose was removed and cut into four 30 - 40 cm and one 5 cm section. Biofilm in the 30 to 40-cm sections was collected using a biofilm sampler consisting of a silicone plug matching the internal diameter of the pipe and a 50-cm stainless steel rod (Fig. S4). The sampler was rinsed with phosphate buffer solution (PBS, pH = 7.2), and the rinse solution was collected. This process was repeated three times. Four sections of shower hose biofilm were collected in the same sterile 50 mL centrifuge tube (pooled as one sample), and the final biofilm suspension volume was 50 mL, which was thoroughly vortexed and shaken for further microbiological analysis. For the 5 cm section used for biofilm morphology study, the two open ends were sealed with sterile plugs, and the tube was filled with PBS. It is important to mention that the biofilm sampling for SHD was different. The biofilm from SHD were sampled on cotton swab, DNA was extracted for further analysis, but no subsequent biomass measurements nor biofilm characterization were performed.

Similarly, the cold-water pipe (CWP) and hot-water pipe (HWP) were cut into three 30 - 40 cm sections (pooled as one sample in the end) and one 5 cm section. The above-mentioned sampling steps were performed. Biofilm samples were collected in duplicates for SHD, SHE, CWP, and HWP at each temperature setting. All samples were stored at 4 °C and processed within 24 h of collection.

In total, over the period of 40 weeks (W), 312 samples were collected, including 120 water samples and 192 biofilm samples. For

water samples, n = (4 temperatures × 6 sampling times × [(2 water types × 2 replicates) + 1 fresh water] = 120; while for biofilm samples, n = (4 temperatures × 6 sampling times × 4 biofilm types × 2 replicates) = 192.

2.3. Water physicochemical analysis

For all water samples, residual chlorine and total chlorine were measured immediately after sampling using a DR300 spectrophotometer (HACH). Temperature was measured with a multifunctional online monitoring meter. The disinfectant and temperature of the water samples at each sampling event are summarized in Table S2. For FHW samples, total organic carbon (TOC) was determined using a TOC analyzer (Shimadzu, Japan). The concentrations of calcium (Ca) and magnesium (Mg) were analyzed by inductively coupled plasma optical emission spectroscopy (ICP-OES, Shimadzu, Japan). The concentrations of iron (Fe), manganese (Mn), and aluminum (Al) were analyzed by inductively coupled plasma mass spectrometry (ICP-MS, Thermo Fisher Scientific, USA). The concentrations of chloride (Cl^-), sulfate (SO_4^{2-}), and nitrite (NO_3^-) ions were analyzed by ion chromatography (IC, Dionex, USA). The concentration of bicarbonate ions (HCO_3^-) was determined by titration with an acid-base indicator. The physicochemical characteristics of the FHW samples at each sampling event are summarized in Table S3.

2.4. Adenosine triphosphate (ATP) and total cell count (TCC)

Total adenosine triphosphate (ATP) concentrations were quantified to assess the active biomass (Yao et al., 2024). Flow cytometry (FCM) was used to determine total cell counts (TCC) in the water and biofilm suspensions (Neu et al., 2018; Proctor et al., 2018). Detection methods are detailed in Supporting Information (Text S2).

2.5. Biofilm structure analyses with SEM and CLSM

Biofilm structure was visualized by scanning electron microscopy (SEM; FEI Quattro S, USA) (Yao et al., 2024). The distribution of extracellular polymeric substances (EPS) within biofilms was characterized in situ using confocal laser scanning microscopy (CLSM; TCS SP8 CSU, Leica, Germany), as previously described (Chen et al., 2007; Yang et al., 2022). The detailed methodology for biofilm structural analysis is provided in the Supporting Information (Text S3, Table S4).

2.6. Quantitative polymerase chain reaction

The *mip* gene of *Legionella pneumophila* and the *atpE* genes of *Mycobacterium* spp. were targeted via quantitative real-time polymerase chain reaction (qPCR) on a Quant Gene 9600 Real-Time PCR instrument (Bioer, China), following previously published methods (Waak et al., 2018, 2019). Briefly, the qPCR reactions consisted of 10.0 μL of SsoAdvanced Universal Probes Supermix (Bio-Rad), appropriate concentrations of forward and reverse primers and probes (Sangon Biotech, China), 2.0 μL of DNA template, and DNase/RNase-free water (TaKaRa) to a final volume of 20.0 μL. Full primer/probe sequences, PCR reaction concentrations, and thermoprofiles are provided in Table S5. The oligonucleotides used to create the qPCR standard curves are summarized in Table S6. Each qPCR run included standard curves (seven serial dilutions: 10^1 copies/μL to 10^7 copies/μL), negative controls, and samples. Each standard, negative control, and sample was assayed in triplicate (n = 3). The limit of quantification (LOQ) for the qPCR reactions targeting the *mip* and *atpE* genes was 10 copies per reaction. Amplification efficiencies, LOQs, and standard curves are summarized in Table S7. The CT values and the corresponding gene copy number (copies/μL) are summarized in Table S8.

2.7. DNA extraction and sequencing

For FHW and SHW samples, 2 L of water was filtered through 0.2 μm polycarbonate membrane filters (Whatman, UK) for DNA extraction, and 0.2 L of FHW was used for physicochemical and biomass analyses and 0.2 L of SHW was used for biomass analyses. For SGW samples, 200 mL (39 °C) or 450 mL (45, 51, and 58 °C) of water was filtered for DNA extraction, and 50 mL of water was used for biomass analyses. For CWP, HWP, and SHE biofilm samples, 45 mL of biofilm suspension was filtered for DNA extraction, and 5 mL of biofilm suspension was used for biomass analysis. The sterile rayon swabs (Copan, Brescia, Italy) were used to collect biofilms from the holes in the showerhead. The filters and sterile rayon swabs were stored in sterile centrifuge tubes at −20 °C for subsequent DNA extraction. DNA was extracted using the FastDNA Spin Kit for Soil (MP Biomedicals, USA), following the manufacturer's instructions.

For 16S rRNA gene amplicon sequencing, the V3-V4 regions were amplified using the primers 341F (5′-CCTACGGGNGGCWGCAG-3′) and 785R (5′-GACTACHVGGGTATCTAATCC-3′) (Chen et al., 2022). PCR products were purified and prepared for sequencing on an Illumina NovaSeq platform (Shanghai, China) to obtain paired-end 2 × 250 bp reads. A total of 27 samples showed no PCR product bands and were therefore not sequenced. The raw sequences were initially processed with Figaro v1.1.2 to determine trimming parameters (Sasada et al., 2020). Quality filtering, primer removal, error rate learning, sample inference, redundancy removal (duplicate sequences), paired read merging, amplicon sequence variant (ASV) table construction, and chimera removal were performed using DADA2 v1.21.0, resulting in the final ASV table (Callahan et al., 2016). Taxonomic classification was conducted using SILVA 138.1 (Quast et al., 2013), and phylogenetic reconstruction was performed with QIIME2 2021.1 (Bolyen et al., 2019). The sequencing data were deposited in the NCBI database under the reference code PRJNA1249929.

2.8. Statistical analysis

Alpha and beta diversity. Alpha diversity was assessed using the Observed and Shannon indices. Principal Coordinates Analysis (PCoA) was performed based on the Bray-Curtis dissimilarity metric to analyze bacterial community composition. Significant differences in community composition among different groupings were evaluated using permutational multivariate analysis of variance (PERMANOVA) ($p < 0.05$).

SourceTracker analysis. To quantify the contribution of potential sources to the sink, the Bayesian-based SourceTracker method was applied (Knights et al., 2011). In this study, the bacteria in SHW or SGW at each sampling time were considered sinks, while the communities of biofilms (CWP, HWP, SHE, SHD) and FHW were defined as potential sources. Source apportionment was conducted using SourceTracker (V 1.0.1) with default settings, a rarefaction depth of 1000, burn-in of 100, restart of 10, alpha1 of 0.001, alpha2 of 0.1, and beta of 0.01. The analysis was repeated in triplicate, and the average was calculated as previously described (Fang et al., 2023).

Null model analysis. To infer community assembly processes, we calculated the mean nearest taxon distance (MNTD) using the picante R package (Kembel et al., 2010) and applied a null model (1000 permutations) to compute β-nearest taxon index (βNTI) (Stegen et al., 2012; Zhou and Ning, 2017). Thresholds were interpreted as: βNTI > 2 (variable selection), βNTI < −2 (homogeneous selection), and |βNTI| < 2 (stochastic processes). This analytical framework enabled robust differentiation between deterministic environmental filtering and stochastic forces shaping microbial community structure.

Other analysis. Variation partitioning analysis (VPA) was conducted using the R package vegan to assess the relative contributions of temperature, incubation time, freshwater temperature, and residual chlorine to the bacterial community. Linear discriminant analysis effect size (LEfSe) was applied to identify the most significantly enriched ASVs

in response to selected factors, with a significance threshold of > 4.

3. Results

3.1. Development of biomass in shower system

The development of biomass in shower systems was shown in ATP (Fig. 1) and TCC (Fig. S5). In general, all biofilm exhibited high biomass at 4th-week, followed by significant decreases and another wave of increases, with the highest biomass observed in shower hoses (SHE: 455.1 $\pm$ 381.3 pg ATP/cm^2; 3.0 $\pm$ 2.4 $\times$ 10^5 cells/cm^2), followed by cold-water pipes (CWP: 7.6 $\pm$ 2.0 pg ATP/cm^2; 2.0 $\pm$ 1.1 $\times$ 10^4 cells/cm^2), and hot-water pipes (HWP: 3.5 $\pm$ 3.7 pg ATP/cm^2; 2.0 $\pm$ 1.1 $\times$ 10^4 cells/cm^2). This trend of peak biomass at the early stage (4th-week) and the following sharp decreases may be because the leaching of organic matter from plastic pipe material promoted the fast growth of attached microbes, which faded away and washed out accompanied by the observed decrease of biomass (Fig. S3).

Specifically, for CWP, the biomass decreased from 4th-week to 10th-week (8.5 $\pm$ 1.7 to 5.2 $\pm$ 1.6 pg ATP/cm^2), steadily increased till 30th-week, and then decreased till 40th-week (Fig. 1A). For HWP, the biomass dropped from 4th-week to 16th-week (4.9 $\pm$ 3.1 to 2.0 $\pm$ 2.0 pg ATP/cm^2), gradually increased till 30th-week, and then decreased till 40th-week (Fig. 1B). For SHE, the biomass decreased from 4th-week to 10th-week (711.6 $\pm$ 324.4 to 153.1 $\pm$ 52.7 pg ATP/cm^2), steadily decreased till 22nd-week, then sharply increased at 40th-week (969.5 $\pm$ 143.4 pg ATP/cm^2) (Fig. 1C).

For heating temperatures, contrary influences were observed for CWP and HWP. The biomass was the lowest at 39 °C in CWP (5.2 $\pm$ 1.3 pg ATP/cm^2) and increase with the increase of temperature. This phenomenon may be attributed to prolonged stagnation in CWP when the water heater temperature was set at 39 °C, which prevented nutrient replenishment from fresh water. For HWP, the highest biomass was observed at 39 °C (9.2 $\pm$ 2.3 pg ATP/cm^2), which decreased with the decrease of temperature. It can be explained by the inhibition of biofilm by heating. Interestingly, the biomass was the lowest in SHE with heating temperature set at 45 °C, with the rest of the temperatures not significantly different from each other, indicating 45 °C might be an optimal heating temperature from the biomass perspective.

For water (Fig. 1D-F and S5D-F), the highest biomass was observed in stagnant water (SGW: 31.9 $\pm$ 22.3 pg ATP/mL; 5.3 $\pm$ 2.6 $\times$ 10^4 cells/mL), while the biomass in shower water (SHW: 12.0 $\pm$ 7.7 pg ATP/mL; 1.9 $\pm$ 1.1 $\times$ 10^4 cells/mL) and fresh water (FHW: 12.8 $\pm$ 8.0 pg ATP/mL; 1.8 $\pm$ 1.2 $\times$ 10^4 cells/mL) was not significantly different. This indicates that the potential risks in SGW would be the highest compared to SHW and FHW. Moreover, the changes in water corresponded well to biofilm (Fig. 1A-C).

3.2. Biofilm morphology and structure

Biofilm morphology and structure was characterized by SEM (Fig. S6A1-C6) and CLSM (Fig. S6A-C). In general, the SEM - observed changes of biofilm quantity over time were consistent with the alterations in ATP concentration presented above. For example, the number of microorganisms was higher in SHE than in CWP and HWP. Besides, the extracellular polymeric substances (EPS) of biofilm (40th-week) were characterized by CLSM (Fig. S6A-C). The picture showed that the EPS of biofilm in CWP and HWP were thin and sparsely distributed, while the EPS in SHE was thicker and more clustered than CWP and HWP. Within EPS of all pipes, total proteins exhibited the strongest fluorescence intensity, followed by α-polysaccharide, β-polysaccharide, and lipids.

3.3. Bacterial community diversity

Alpha diversity. Temporal changes in the number of observed ASVs are shown in Fig. S7. Among biofilms, SHD exhibited the highest ASV richness (102 $\pm$ 16), followed by CWP (80 $\pm$ 17), HWP (72 $\pm$ 28), and SHE (35 $\pm$ 12), mirroring trends in the Shannon index. ASV counts increased over time in all biofilms except SHE. In water samples, shower water (SHW) consistently showed higher ASV numbers (148 $\pm$ 20) than fresh water (FHW, 115 $\pm$ 19), suggesting microbial transfer from biofilms to the shower water. In contrast, stagnant water (SGW) had the lowest richness (64 $\pm$ 15), indicating species loss during stagnation. Heating temperature had no significant effect on alpha diversity in either biofilm or water communities (Fig. S8).

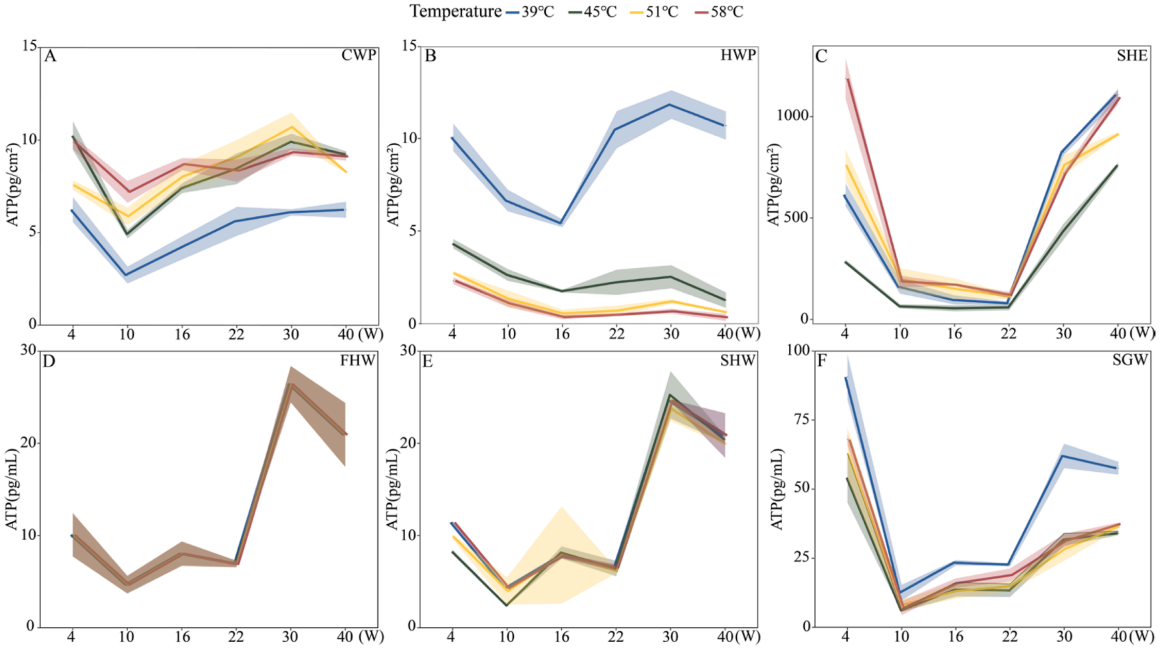

Fig. 1. The ATP of biofilm and water over forty weeks. ATP concentration variations in CWP (A), HWP (B), SHE (C), FHW (D), SHW (E), and SGW (F) at different temperatures (39, 45, 51 and 58 °C). Line plots represent mean values with error bands (mean $\pm$ std.).

Beta diversity. Overall, bacterial communities from different phases clustered distinctly (Fig. S9). Biofilms in CWP and HWP were similar, as were fresh and shower water, while microbial communities in stagnant water (SGW) resembled those in shower hoses (SHE). During the first 22 weeks, SHD formed a separate cluster but became more similar to HWP from 30th-week onwards. The biofilms of same age clustered more closely than those with the same temperature, indicating dynamic microbial community shifts over time (Fig. 2A–D). Specifically, in CWP and HWP, microbial communities at different temperatures were more alike at 4th-week and distinct from other time points, likely due to initial DOC release from pipes promoting selective microbial growth. Samples from 10th- and 16th-week, and from 30th-week and 40th-week, also clustered together. In SHE, microbial communities remained relatively consistent across time. In SHD, 4th- to 16th-weeks were similar, while 22nd-week formed a separate cluster, and 30th- and 40th-week clustered together.

Temperature significantly influenced bacterial communities in both CWP (adonis, $p < 0.001$; betadisper, $p = 0.06$) and HWP (adonis, $p = 0.013$; betadisper, $p = 0.17$) (Fig. 2A, 2B). In CWP, prolonged stagnation at 39 °C led to a distinct microbial community. Bray-Curtis distances were lower between CWP samples at the same temperature, highlighting a strong temperature effect (Fig. S10A). In contrast, HWP showed similar within- and between-temperature distances, suggesting greater temporal variability (Fig. S10B). Notably, inter-temperature distances increased with runtime (Fig. 2E), indicating that temperature effects on biofilm development intensified over time. Temperature also affected microbial communities in SHE (adonis, $p = 0.022$; betadisper, $p = 0.005$) (Fig. 2C, S10C), but not in SHD (adonis, $p = 0.84$) (Fig. 2D, S10D).

Biofilm community assembly. The null model analysis revealed that stochastic processes dominated throughout the 40-week biofilm development period. Notably, deterministic processes began to emerge after week 30 in both CWP and SHE (Fig. S11A-B), while appearing earlier (post-week 22) in HWP (Fig. 2F). In contrast, deterministic processes persisted consistently throughout the entire observation period in SHD (Fig. S11C). VPA results were shown in Fig. 2G-J, illustrated that the temperature of fresh water and residual chlorine accounted for the largest variation (11–38 %), followed by incubation time (10–18 %) and heating temperature (0–15 %).

3.4. Bacterial community composition

Bacterial community analysis revealed the top 20 dominant genera in terms of relative abundance across different temperatures, incubation

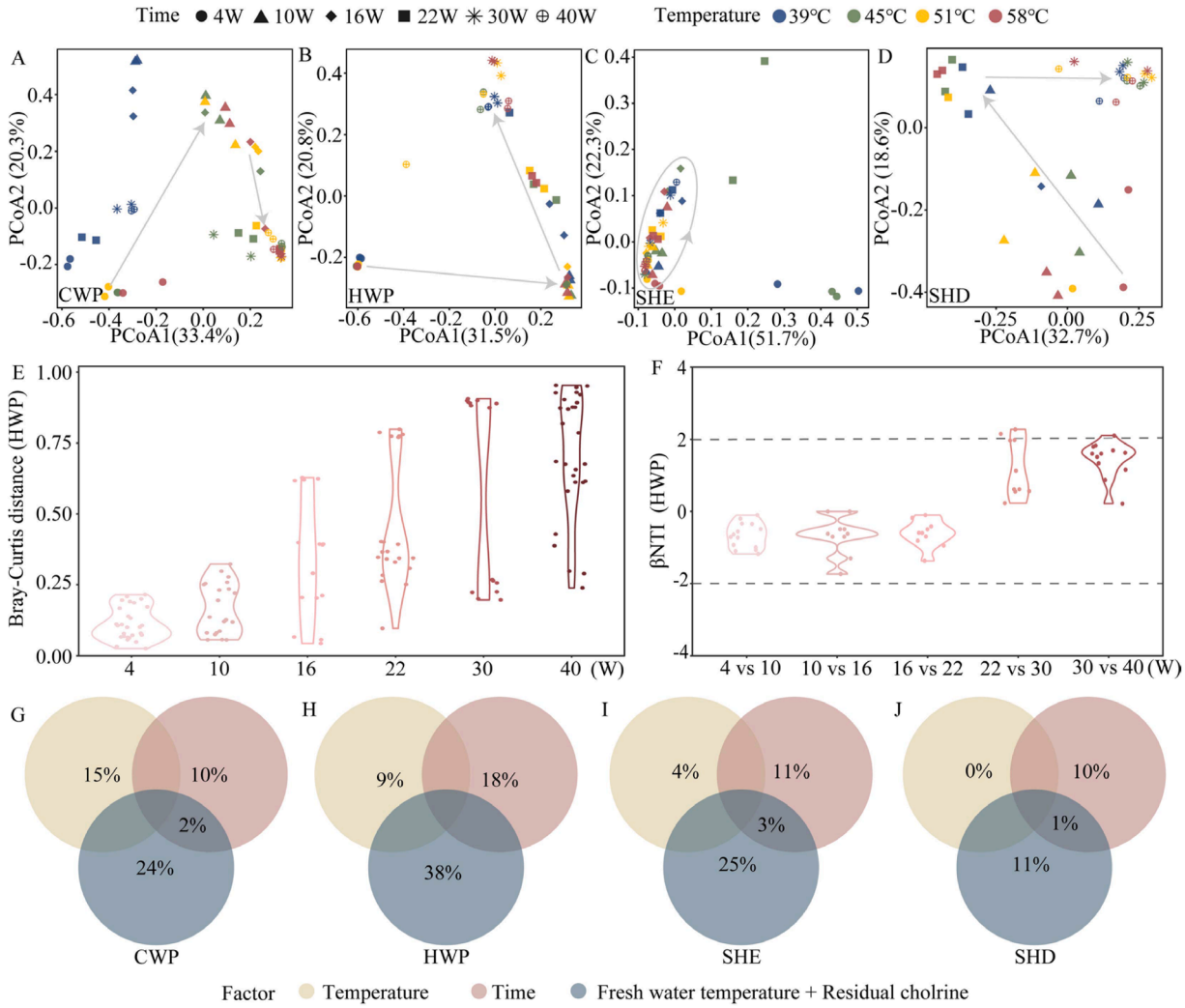

Fig. 2. Beta diversity of the bacterial communities of biofilms. Principle coordinate analysis (PCoA) plots illustrate the beta diversity of bacterial communities of biofilms under different temperatures over time in (A) Cold water pipes, CWP; (B) Hot water pipes, HWP; (C) Shower hoses, SHE; and (D) Shower heads, SHD. Bray-Curtis distances between HWP biofilm at same age but different temperatures over time (E) the dynamics of HWP biofilm inβNTI values over time. Dashed grey lines indicate the assembly process thresholds: βNTI < -2 represents homogenous selection, βNTI > 2 indicates variable selection, and $|$βNTI$| < 2$ indicates stochastic assembly. (F) Variation partitioning analysis highlights the relative contributions of temperature, time, fresh water temperature, and residual chlorine to beta diversity in CWP biofilm (G), HWP biofilm (H), SHE biofilm (I), and SHD biofilm (J).

times, and phases. In Biofilms, the dominant genera change over time and space. Both CWP and HWP were initially dominated by G9 (*Caulobacter*) and G18 (*Ferrovibrio*) at 4th-week (Fig. 3A–B). By the 10th-week, G4 (*Ralstonia*) and G14 (*Acidovorax*) became dominant, with G4 remaining dominant at the 16th-week. After the 22nd-week, the dominant genera diverged between CWP and HWP, especially across temperatures. In CWP at 45, 51, and 58 °C, G3 (*Phreatobacter*), G12 (Obscuribacteraceae), and G17 (Hyphomonadaceae) dominated from the 22nd-week onward. Differently, at 39 °C, G7 (*Novosphingobium*) and G9 (*Caulobacter*) dominated at the 22nd-week, and G6 (Sphingomonadaceae) at 30th- and 40th-week. While in HWP (45–58 °C), G19 (*Dietzia*) and G4 (*Ralstonia*) dominated at the 22nd-week; G5 (*Rhodococcus*) and G21 (Micrococcaceae) at the 30th-week; and G5 with G8 (*Blastomonas*) at the 40th-week. At 39 °C, G3 (*Phreatobacter*) remained dominant from the 22nd-week onward. Overtime, G1 (*DSSF69*) consistently dominated in SHE (Fig. 3C), and the dominant genera in SHD included G5, G7, G8, and G11 (*Mycobacterium*) (Fig. 3D).

In freshwater (FHW), G3 (*Phreatobacter*) was dominant at the 4th-week, replaced by G2 (Chloroplast) after the 10th-week (Fig. S12). In shower water (SHW), both G3 (*Phreatobacter*) and G1 (*DSSF69*) were dominant at 39 °C at the 4th-week, while only G1 remained dominant at 45–58 °C. After 10th-week, G2 (Chloroplast) became dominant. In stagnant water (SGW), G1 (*DSSF69*) was consistently dominant overtime.

LEfSe Analysis. The ASVs significantly enriched at different time and spot were identified and shown in Fig. 3E and Table S9. At the 4th-week, ASV8 (*Caulobacter*), ASV14 (*Ferrovibrio*), ASV20 (*Delftia*), ASV25 (*Curvibacter*), and ASV37 (Rhizobiaceae) were abundant in CWP and HWP but declined or disappeared over time. In contrast, ASV3 (*Phreatobacter*) increased in both systems—from 10 % to 32 % in CWP, and from 0.7 % to 17 % in HWP from the 4th to the 40th-week. ASV1 (*DSSF69*) maintained high abundance in SHE (70–91 %). In SHD, ASV18 (*Mycobacterium*) declined from 5 % (4th-week) to 0 % (22nd-week), then rose to 7–8 % (30th- and 40th-week). ASV5 (*Rhodococcus*) and ASV22 (*Aquabacterium*) showed similar patterns.

3.5. Source apportionment of microbes in shower and stagnant water

At the 4th-week, shower water (SHW) microbes were primarily originated from fresh water (FHW, 2 %–65 %) and shower hose biofilm (SHE, 28 %–95 %), while after 10th-week, FHW (50 %–95 %) became the dominant source (Fig. 4A). Temperature played a key role at the 4th-week: in SHW at 39 °C, FHW contributed 65 % and SHE 28 %, whereas at 45–58 °C, FHW accounted for only 2 %–20 % and SHE 47 %–95 %, aligning with microbial community shifts (Fig. S12B). For stagnant water, SHE consistently dominated across all conditions (52 %–95 %) (Fig. 4B). In fact, *DSSF69* spp. showed high relative abundance in SGW (39 %–94 %) and dominated in SHE (45 %–98 %). Shower head (SHD) was the second-largest source for both SHW (1 %–41 %) and SGW (1 %–40 %). Notably, the FHW-derived microbes were largely replaced by biofilm, particularly from SHE and SHD, underscoring the strong impact of biofilms on stagnant water communities.

3.6. Quantification of selected marker genes biofilm

Legionella pneumophila. As shown in Fig. 5A, L. *pneumophila* concentrations varied significantly over space and time ($p < 0.05$). The shower head (SHD) showed the highest concentrations over the 40-week period, with 24/35 samples positive and an average of $5.1 \pm 9.8 \times 10^4$ copies/cm^2. This was followed by cold water pipe (CWP, 26/48, $2.0 \pm 9.4 \times 10^3$ copies/cm^2), shower hose (SHE, 21/47, $1.4 \pm 1.0 \times 10^2$ copies/cm^2), and hot water pipe (HWP, 25/42, $1.0 \pm 1.5 \times 10^2$ copies/cm^2). The detection rates were highest at the 4th-week and after the 22nd-week. At the 4th-week, low concentrations ($< 10^2$ copies/cm^2) were detected in 2/8 CWP, 6/8 HWP, 2/8 SHE, and 0 SHD. At the 10th-week, L. *pneumophila* was undetectable in CWP, HWP, and SHE, while at the 22nd-week it was detected in 28/30 biofilm samples (up to 3.8×10^4 copies/cm^2), which further increased by the 40th-week (30/31 samples, up to 4.9×10^4). Notably, shower head (SHD) showed early detection at the 10th-week (2/8) and remained consistently positive thereafter. Among temperatures, the highest L. *pneumophila* concentrations were detected at 39 °C, while other temperatures showed no significant differences, suggesting 39 °C may favor its growth.

***Mycobacterium* spp.** Similar to L. *pneumophila*, the highest concentrations of *Mycobacterium* spp. were found in SHD (27/35, $1.2 \pm 2.5 \times 10^4$ copies/cm^2) (Fig. 5B), followed by SHE (2/47, $7.7 \pm 2.5 \times 10^2$ copies/cm^2), CWP (26/48, $1.4 \pm 3.5 \times 10^2$ copies/cm^2), and HWP (25/42, $0.2 \pm 0.2 \times 10^2$ copies/cm^2). *Mycobacterium* spp. was not detected CWP, HWP, and SHE until the 22nd-week. After the 30th-week, it was detected in 12/16 CWP, 14/14 HWP, and 2/15 SHE. Differently, SHD tested positive since the 4th-week (3/3), with a decreasing detection rate till the 22nd-week (1/8) but remained positive in all samples after the 30th-week. Interestingly, only one CWP sample at 39 °C tested positive, with a very low concentration, suggesting that *Mycobacterium* spp. may not thrive in long-term stagnant conditions.

4. Discussion

This study is among the first to systematically track dynamic changes in biomass, microbial diversity, community composition, and opportunistic pathogens across shower biofilms (cold-water pipe, hot-water pipe, shower hose, shower head) and water phases (fresh, shower, and stagnant) under varying temperatures. By assessing all components and phases of the shower system, we identified both temporal and spatial hotspots of potential microbial risk.

4.1. Initial biofilm exhibits peak biomass, unique community, and high loss

We observed an initial biofilm peak at the 4th-week, characterized by elevated ATP, TCC, and microbial density in SEM images (Fig. 1, S5, S6), which declined by the 10th–22nd week, followed by regrowth up to the 40th-week. This pattern aligns with previous studies reporting high initial biomass on plastic pipes that subsequently decreased over 4–16 weeks (Learbuch et al., 2021). The initial surge is attributed to the leaching of organic matter from plastic materials, which promotes microbial growth (Ren et al., 2023; Romera-Castillo et al., 2018; Sheridan et al., 2022). Notably, Wen et al. and Bucheli-Witschel et al. (Bucheli-Witschel et al., 2012; Wen et al., 2015) documented rapid declines in leached organics (e.g., total and assimilable organic carbon), consistent with the sharp biofilm reduction observed after the 4th-week in this study. Our 7-day simulated pipe leaching experiment also confirmed that CWP, HWP, and SHE all release TOC, with leaching rates decreasing over the incubation period (Text S1 and Figure S3). Coincidently, the residual chlorine concentration significantly increased from 0.44 ± 0.04 mg/L at 4th-week to 0.76 ± 0.03 mg/L at 10th-week, and high residual chlorine concentrations are known to inhibit microbial growth (Butterfield et al., 2002; Oliveira et al., 2024). However, CWP (39 °C) experienced long-term stagnation, meaning that changes in residual chlorine did not affect CWP (39 °C), yet the ATP concentration still decreased by 56.6 %. Thus, we suggest that the initial release of DOC from the plastic pipe is the primary cause of the high biofilm biomass at 4th-week. The subsequent regrowth of biofilm up to the 40th-week is likely fueled by nutrients in the supplied water. This shift corresponds to the marked differences in microbial community structures observed between weeks 4 and 40 across all pipe types and temperatures (Brislawn et al., 2019; Douterelo et al., 2018; Pinto et al., 2019; Zhang et al., 2019). For example, the microbial community was unique at 4 weeks, regardless of the stagnation conditions and temperature, the *Caulobaeter* spp. and *Ferrovibrio* spp. dominated for all CWP and HWP.

SEM analysis revealed that early-stage (4th-week) biofilms were

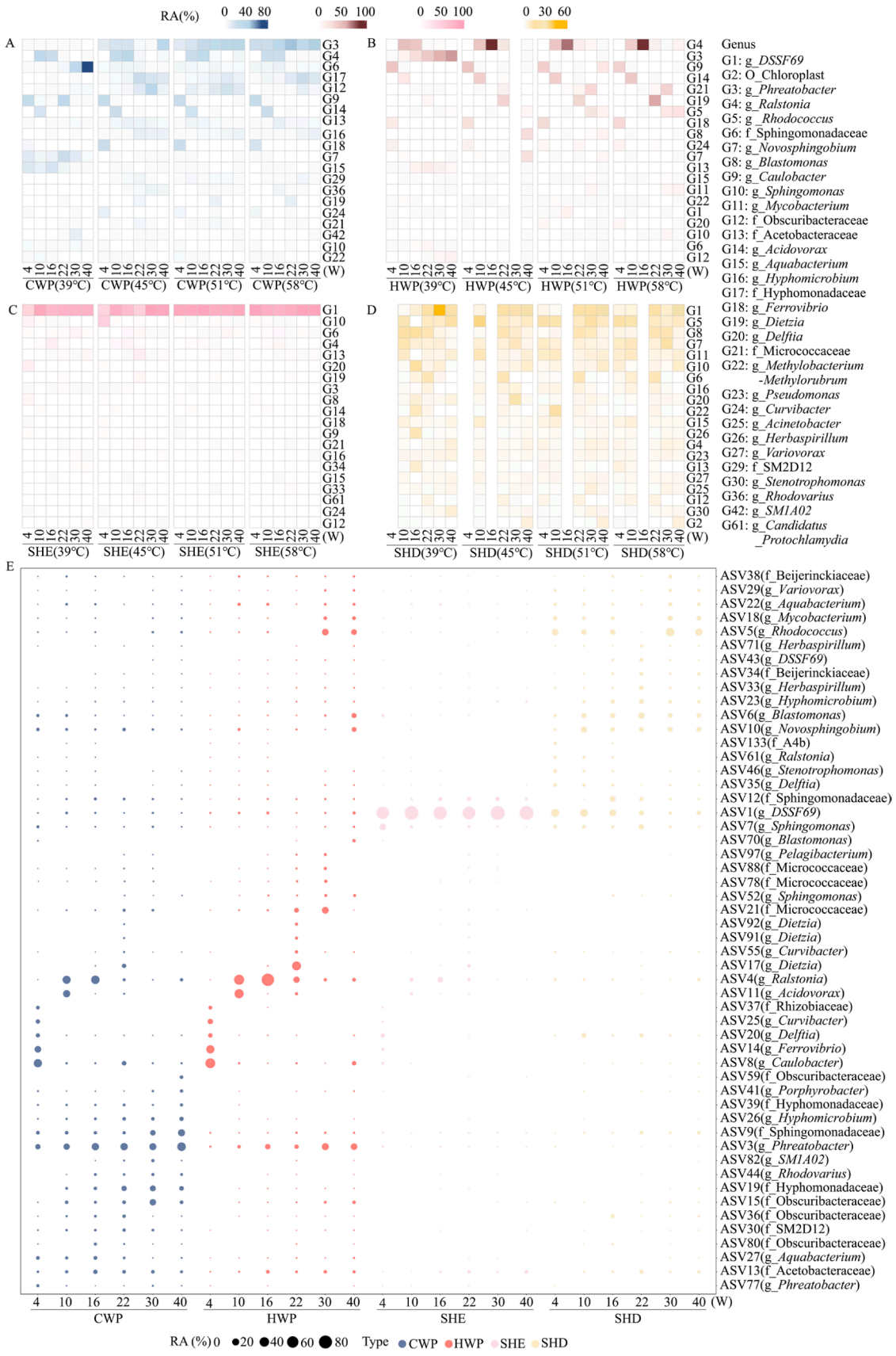

Fig. 3. Bacterial community composition of biofilms. The temporal variation in the relative abundances of top 20 genera in the biofilms of cold-water pipes (CWP, A), hot water pipes (HWP, B), shower hoses (SHE, C), and shower heads (SHD, D). The variations in the relative abundance of sensitive ASVs enriched in the different biofilms over time (i.e., CWP, HWP, SHE, SHD, E), highlighting the spatial and temporal shifts in community composition. The six blank columns correspond to lost samples.

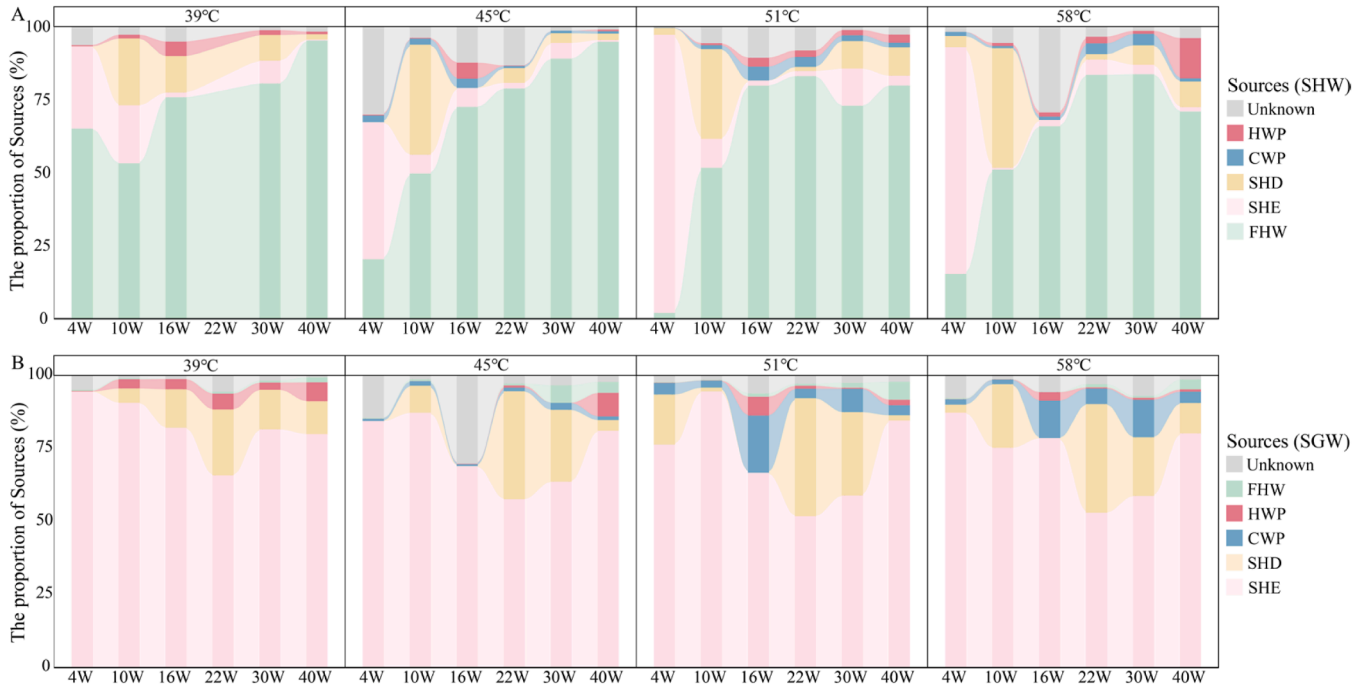

Fig. 4. Sources apportioned by SourceTracker. The percentage contribution of biofilm in CWP, HWP, SHE, SHD and FHW to the microbes in shower water (SHW, A) and stagnant water (SGW, B) across time (4th, 10th, 16th, 22nd, 30th, and 40th week) and temperature (39, 45, 51 and 58 °C).

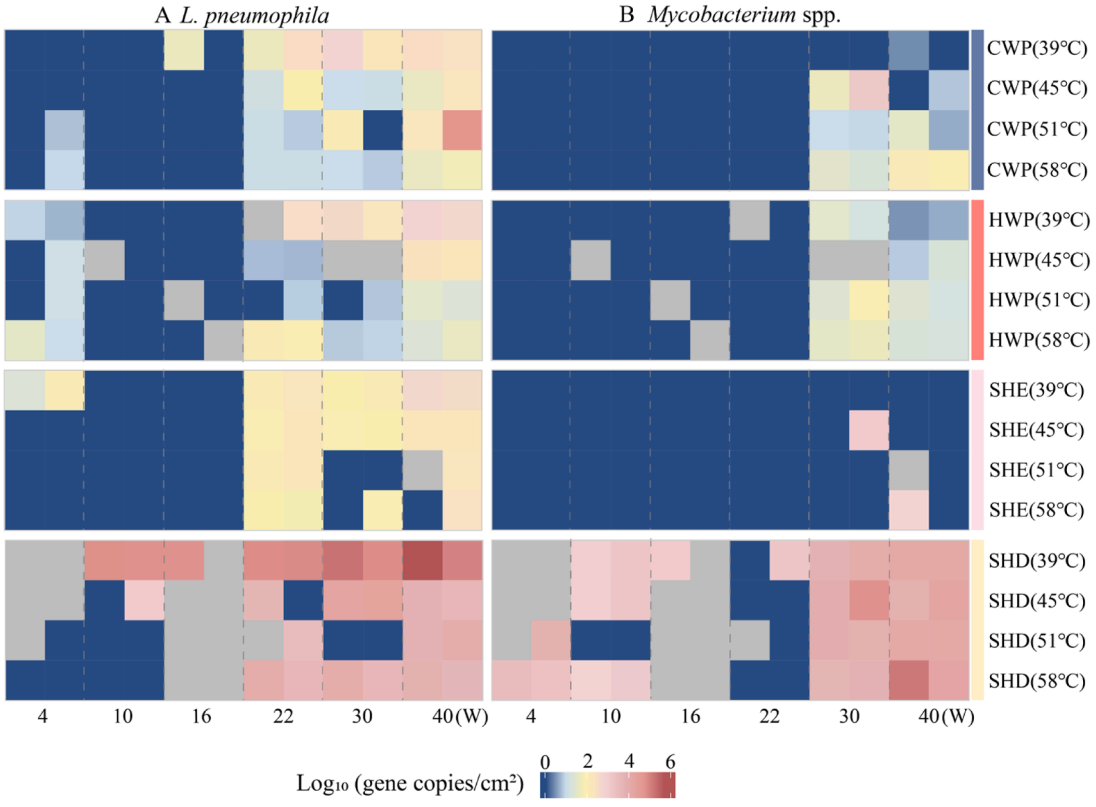

Fig. 5. Heatmap of L. pneumophila (A) and Mycobacterium spp. (B) in biofilms. The figures illustrated the spatial and temporal variations of selected marker genes (gene copies/cm^2) in the biofilms of cold-water pipe (CWP), hot-water pipe (HWP), shower hose (SHE), shower head (SHD) at different incubation times (4th, 10th, 16th, 22nd, 30th, and 40th week) and temperatures (39, 45, 51, and 58 °C). Data were $\log_{10}(x+1)$ transformed. The gray box indicates lost sample.

loosely structured, suggesting greater potential for detachment. This was supported by source tracking, which showed that 62.0 ± 26.1 % of microbes in shower water originated from the shower hose biofilm at the 4th-week, compared to just 1.5 ± 1.2 % at the 40th-week. Shower hose biofilms are of particular concern due to their propensity to support opportunistic pathogens and their high potential for aerosolization

during use (Proctor et al., 2018; Wang et al., 2022; Zhao et al., 2024). Our findings underscore the elevated microbial and exposure risks associated with the initial stages of shower system installation and operation, driven by organic leaching and the rapid growth and sloughing of biofilm biomass.

4.2. Temporal and spatial hotspots for L. pneumophila and mycobacterium spp

Temporally, L. *pneumophila* followed the same trend as biofilm biomass: it first appeared at the 4th-week in low abundance and detection rates, disappeared for a period, and re-emerged with significantly higher levels from the 22nd-week onward. This aligns with previous findings that L. *pneumophila* is fastidious, requiring L-cysteine and ferric pyrophosphate for growth (R et al., 1980; Wadowsky and Yee, 1983), which can persist in biofilms by utilizing bacterial metabolites and lysed cells (Taylor and Bentham, 2009), with its presence often coinciding with biofilm peaks (Abu Khweek and Amer, 2018; Shrout and Nerenberg, 2012). In contrast, *Mycobacterium* spp. was undetected in all biofilms until the 30th-week, after which its abundance steadily increased—except in SHD, where it was consistently present. This aligns with its known traits: a lipid-rich, hydrophobic outer membrane (Brennan, 1995) that enhances surface adhesion (Bendinger et al., 1993; Pereira et al., 2020), and the ability to metabolize recalcitrant carbon compounds (Wang et al., 2013) and heavy metals (Erardi et al., 1989; Meissner and Falkinham, 1984). However, their slow growth and poor competitiveness in nutrient-rich conditions (Iii, 2009) likely explain their absence in early-stage biofilms (i.e., 4th-week) and later emergence under more selective conditions. Furthermore, previous studies have shown that amoebae prefer to colonize biofilms with sufficient microbial biomass (Goudot et al., 2012). As hosts for L. *pneumophila* and *Mycobacterium* spp., amoebae are positively correlated with the positive detection rates of these pathogens (Marciano-Cabral et al., 2010; Thomas et al., 2014). Regrettably, quantitative analysis of amoebae was not included in our study design.

Spatially, both L. *pneumophila* and *Mycobacterium* spp. were significantly enriched in showerhead biofilms (SHD), with L. *pneumophila* concentrations 384-, 558-, and 519-fold higher than in SHE, CWP, and HWP, respectively; *Mycobacterium* spp. showed 21-, 442-, and 764-fold increases. Prior studies also reported significant enrichment of opportunistic pathogens in showerheads (Feazel et al., 2009). For instance, one study using ITS gene sequencing found *Mycobacterium* sequences in showerhead biofilms were 100 times more abundant than in background water. In contrast, our study applied qPCR to quantify L. *pneumophila* and *Mycobacterium* spp. across pipe types, revealing clear spatial hotspots. The showerhead's high surface-to-volume ratio, exposure to air, warm water (~39 °C), low residual chlorine, and conducive structure for scale and biofilm buildup create an ideal environment for pathogen persistence (Proctor et al., 2018). Additionally, the semi-moist conditions, turbulent shear flow, and rapid temperature shifts (Gebert et al., 2018) likely favor slow-growing microbes like L. *pneumophila* and *Mycobacterium* spp., which are well-adapted to survive desiccation and environmental fluctuations (Falkinham et al., 2015; Proctor et al., 2022).

4.3. Implications and outlook

We identified temporal and spatial hotspots of microbial risk in shower systems, offering insights for effective user-end management. Early-stage (4-week) biofilms exhibited high biomass with easily detached cells and detectable L. *pneumophila*, a risk reducible by presoaking pipes before use, whereas prolonged use (>22 weeks) led to significant pathogen accumulation (L. *pneumophila* and *Mycobacterium* spp.), necessitating timed interventions.

The influence of temperature on microbial communities became more pronounced over time, likely masked early on by DOC leaching from plastic materials. This emphasizes the importance of long-term monitoring, as short-term studies may underestimate pathogen risks and overlook temperature effects. Showerheads and hoses emerged as key hotspots, with the highest concentrations of L. *pneumophila* and *Mycobacterium* spp. found in showerheads, and the second highest in hoses. Unlike embedded pipes, these components are easy to access, clean, or replace. Regular maintenance—particularly after 22 weeks—can significantly reduce microbial risks.

Moreover, we noted that the positive rates and concentrations of L. *pneumophila* and *Mycobacterium* spp. in the biofilms of CWP are also concerning. To address this, we propose optimizing pipeline design, implementing periodic hot-water flushing of CWP, and installing ultraviolet (UV) disinfection units at the cold water inlets of shower systems to ensure microbial water quality.

5. Conclusions

In summary, this study investigated biofilm development, microbial community dynamics, and opportunistic pathogen presence across shower system components under varying temperatures and incubation periods.

- A sharp biomass peak occurred at the 4th-week, driven by DOC leaching from plastic pipes, particularly in SHE, which exhibited significantly higher biomass than CWP and HWP. Biomass declined by the 10th-week as DOC levels dropped.
- Early biofilms were loosely attached and easily detached, contributing substantially to microbial loads in shower water. Source tracking showed that at the 4th-week, SHW was primarily derived from SHE (28–95 %) and FHW (2–65 %), shifting to FHW (50–95 %) and SHD (1–41 %) at later stages. SGW was consistently dominated by SHE (52–95 %) and SHD (1–40 %).
- L. pneumophila appeared at the 4th-week in low abundance, reemerging and increasing after the 22nd-week. Mycobacterium spp. was detected from the 30th-week onward. Both were highly enriched in showerheads, confirming them as pathogen hotspots.
- This study identifies two critical risk periods: early use and long-term operation. Regular flushing (e.g., heat shock flushing) and timely replacement of showerheads and hoses are effective strategies to reduce microbial risks.

It should be noted that, we used a full-scale shower system under controlled conditions, simulating realistic usage (three 8-minute sessions/week). Unlike field settings, which involve complex, interacting variables (e.g., water chemistry, temperature, disinfectant, usage frequency, materials), our design allowed isolation of specific factors like temperature and time. However, we only tested one pipe material and water-use pattern. Future work should explore the combined effects of water chemistry, disinfectant levels and types, material type, usage frequency, and temperature on microbial communities and pathogen proliferation in real-world settings. Moreover, this study only employed a DNA-based qPCR method to quantify opportunistic pathogens, which cannot distinguish between dead and live bacteria. Future research could utilize culture-based methods to quantify live opportunistic pathogens.

CRediT authorship contribution statement

Anran Ren: Writing – original draft, Visualization, Methodology, Investigation, Conceptualization. **Mingchen Yao:** Methodology, Formal analysis. **Yue Zhang:** Methodology, Formal analysis. **Lihua Chen:** Methodology, Formal analysis. **Xiaoming Li:** Methodology, Formal analysis. **Wei Yan:** Resources, Investigation, Formal analysis. **Walter van der Meer:** Writing – review & editing, Formal analysis. **Joan Rose:** Writing – review & editing. **Gang Liu:** Writing – review & editing, Validation, Supervision, Resources, Project administration,

Methodology, Funding acquisition, Formal analysis, Conceptualization.

Declaration of competing interest

The authors declare that they have no known competing financial interests or personal relationships that could have appeared to influence the work reported in this paper.

Acknowledgments

The present work has been financially supported by the National Natural Science Foundation of China (52370105, 52388101, 52022103).

Supplementary materials

Supplementary material associated with this article can be found, in the online version, at doi:10.1016/j.watres.2025.124028.

Data availability

Data will be made available on request.

References

Abu Khweek, A., Amer, A.O., 2018. Factors mediating environmental biofilm formation by Legionella pneumophila. Front. Cell Infect. Microbiol. 8, 38.
Bendinger, B., Rijnaarts, H.H.M., Altendorf, K., Zehnder, A.J.B., 1993. Physicochemical cell surface and adhesive properties of coryneform bacteria related to the presence and chain length of mycolic acids. Appl. Environ. Microbiol. 59 (11), 3973.
Bolyen, E., Rideout, J.R., Dillon, M.R., Bokulich, N., Abnet, C.C., Al-Ghalith, G.A., Alexander, H., Alm, E.J., Arumugam, M., Asnicar, F., Bai, Y., Bisanz, J.E., Bittinger, K., Brejnrod, A., Brislawn, C.J., Brown, C.T., Callahan, B.J., Caraballo-Rodriguez, A.M., Chase, J., Cope, E.K., Da Silva, R., Diener, C., Dorrestein, P.C., Douglas, G.M., Durall, D.M., Duvallet, C., Edwardson, C.F., Ernst, M., Estaki, M., Fouquier, J., Gauglitz, J.M., Gibbons, S.M., Gibson, D.L., Gonzalez, A., Gorlick, K., Guo, J., Hillmann, B., Holmes, S., Holste, H., Huttenhower, C., Huttley, G.A., Janssen, S., Jarmusch, A.K., Jiang, L., Kaehler, B.D., Bin Kang, K., Keefe, C.R., Keim, P., Kelley, S.T., Knights, D., Koester, I., Kosciolek, T., Kreps, J., Langille, M.G. I., Lee, J., Ley, R., Liu, Y.-X., Loftfield, E., Lozupone, C., Maher, M., Marotz, C., Martin, B.D., McDonald, D., McIver, L.J., Melnik, A.V., Metcalf, J.L., Morgan, S.C., Morton, J.T., Naimey, A.T., Navas-Molina, J.A., Nothias, L.F., Orchanian, S.B., Pearson, T., Peoples, S.L., Petras, D., Preuss, M.L., Pruesse, E., Rasmussen, L.B., Rivers, A., Robeson II, M.S., Rosenthal, P., Segata, N., Shaffer, M., Shiffer, A., Sinha, R., Song, S.J., Spear, J.R., Swafford, A.D., Thompson, L.R., Torres, P.J., Trinh, P., Tripathi, A., Turnbaugh, P.J., Ul-Hasan, S., vander Hooft, J.J.J., Vargas, F., Vazquez-Baeza, Y., Vogtmann, E., von Hippel, M., Walters, W., Wan, Y., Wang, M., Warren, J., Weber, K.C., Williamson, C.H.D., Willis, A.D., Xu, Z.Z., Zaneveld, J.R., Zhang, Y., Zhu, Q., Knight, R., Caporaso, J.G, 2019. Reproducible, interactive, scalable and extensible microbiome data science using QIIME 2. Nat. Biotechnol. 37 (8), 852–857.
Brennan, P.J., 1995. The envelope of mycobacteria. Annu. Rev. Biochem. 64 (1), 29–63.
Brislawn, C.J., Graham, E.B., Dana, K., Ihardt, P., Fansler, S.J., Chrisler, W.B., Cliff, J.B., Stegen, J.C., Moran, J.J., Bernstein, H.C., 2019. Forfeiting the priority effect: turnover defines biofilm community succession. ISME J. 13 (7), 1865–1877.
Bucheli-Witschel, M., Kötzsch, S., Darr, S., Widler, R., Egli, T., 2012. A new method to assess the influence of migration from polymeric materials on the biostability of drinking water. Water Res. 46 (13), 4246–4260.
Butterfield, P.W., Camper, A.K., Ellis, B.D., Jones, W.L., 2002. Chlorination of model drinking water biofilm: implications for growth and organic carbon removal. Water Res. 36 (17), 4391–4405.
Callahan, B.J., McMurdie, P.J., Rosen, M.J., Han, A.W., Johnson, A.J.A., Holmes, S.P., 2016. DADA2: high-resolution sample inference from Illumina amplicon data. Nat. Methods 13 (7), 581-+.
Chen, L., Li, X., van der Meer, W., Medema, G., Liu, G., 2022. Capturing and tracing the spatiotemporal variations of planktonic and particle-associated bacteria in an unchlorinated drinking water distribution system. Water Res. 219.
Chen, M.-Y., Lee, D.-J., Tay, J.-H., Show, K.-Y., 2007. Staining of extracellular polymeric substances and cells in bioaggregates. Appl. Microbiol. Biotechnol. 75 (2), 467–474.
Collins, S., Stevenson, D., Bennett, A., Walker, J., 2017. Occurrence of Legionella in UK household showers. Int. J. Hyg. Env. Health 220 (2), 401–406.
Cordes, L.G., Wiesenthal, A.M., Gorman, G.W., Phair, J.P., Sommers, H.M., Brown, A., Yu, V.L., Magnussen, M.H., Meyer, R.D., Wolf, J.S., Shands, K.N., Fraser, D.W., 1981. Isolation of Legionella pneumophila from hospital shower heads. Ann. Intern. Med. 94 (2), 195–197.
Douterelo, I., Fish, K.E., Boxall, J.B., 2018. Succession of bacterial and fungal communities within biofilms of a chlorinated drinking water distribution system. Water Res. 141, 74–85.
Erardi, F.X., Failla, M.L., Falkinham, I.J.O., 1989. Accumulation and transport of cadmium by tolerant and susceptible strains of mycobacterium scrofulaceum. Antimicrob. Agents Chemother. 33 (3), 350–355.
Falkinham III, J.O., 2011. Nontuberculous mycobacteria from household plumbing of patients with Nontuberculous mycobacteria disease. Emerg. Infect. Dis. 17 (3), 419–424.
Falkinham, J.O., Pruden, A., Edwards, M., 2015. Opportunistic premise plumbing pathogens: increasingly important pathogens in drinking water. Pathogens 4 (2), 373–386.
Fang, J., Dai, Z., Li, X., van der Hoek, J.P., Savic, D., Medema, G., van der Meer, W., Liu, G., 2023. Service-lines as major contributor to water quality deterioration at customer ends. Water Res. 241.
Farhat, M., Moletta-Denat, M., Frere, J., Onillon, S., Trouilhe, M.-C., Robine, E., 2012. Effects of disinfection on Legionella spp., Eukarya, and biofilms in a hot water system. Appl. Env. Microbiol. 78 (19), 6850–6858.
Feazel, L.M., Baumgartner, L.K., Peterson, K.L., Frank, D.N., Harris, J.K., Pace, N.R., 2009. Opportunistic pathogens enriched in showerhead biofilms. PNAS 106 (38), 16393–16398.
Gebert, M.J., Delgado-Baquerizo, M., Oliverio, A.M., Webster, T.M., Nichols, L.M., Honda, J.R., Chan, E.D., Adjemian, J., Dunn, R.R., Fierer, N., 2018. Ecological analyses of mycobacteria in showerhead biofilms and their relevance to human health. MBIO 9 (5).
Gerdes, M.E., Miko, S., Kunz, J.M., Hannapel, E.J., Hlavsa, M.C., Hughes, M.J., Stuckey, M.J., Watkins, L.K.F., Cope, J.R., Yoder, J.S., Hill, V.R., Collier, S.A., 2023. Estimating waterborne infectious disease burden by exposure route, United States, 2014. Emerg. Infect. Dis. 29 (7), 1357–1366.
Goudot, S., Herbelin, P., Mathieu, L., Soreau, S., Banas, S., Jorand, F., 2012. Growth dynamic of naegleria fowleri in a microbial freshwater biofilm. Water Res. 46 (13), 3958–3966.
Hayes-Phillips, D., Bentham, R., Ross, K., Whiley, H., 2019. Factors influencing Legionella contamination of domestic household showers. Pathogens 8 (1).
Iii, J.O.F., 2009. Surrounded by mycobacteria: nontuberculous mycobacteria in the human environment. J. Appl. Microbiol. 107 (2).
Kembel, S.W., Cowan, P.D., Helmus, M.R., Cornwell, W.K., Morlon, H., Ackerly, D.D., Blomberg, S.P., Webb, C.O., 2010. Picante: r tools for integrating phylogenies and ecology. Bioinformatic 26 (11), 1463–1464.
Knights, D., Kuczynski, J., Charlson, E.S., Zaneveld, J., Mozer, M.C., Collman, R.G., Bushman, F.D., Knight, R., Kelley, S.T., 2011. Bayesian community-wide culture-independent microbial source tracking. Nat. Methods 8 (9), 761–U107.
Kunz, J.M., Lawinger, H., Miko, S., Gerdes, M., Thuneibat, M., Hannapel, E., Roberts, V. A., 2024. Surveillance of waterborne disease outbreaks associated with drinking water - United States, 2015-2020. In: Morbidity and Mortality Weekly Report. Surveillance Summaries. Washington, D.C., pp. 1–23, 2002) 73(1).
Learbuch, K.L.G., Smidt, H., van der Wielen, P.W.J.J., 2021. Influence of pipe materials on the microbial community in unchlorinated drinking water and biofilm. Water Res. 194.
Manuel, C.M., Nunes, O.C., Melo, L.F., 2007. Dynamics of drinking water biofilm in flow/non-flow conditions. Water Res. 41 (3), 551–562.
Marciano-Cabral, F., Jamerson, M., Kaneshiro, E.S., 2010. Free-living amoebae, Legionella and mycobacterium in tap water supplied by a municipal drinking water utility in the USA. J. Water Health 8 (1), 71–82.
Martiny, A.C., Jorgensen, T.M., Albrechtsen, H.J., Arvin, E., Molin, S., 2003. Long-term succession of structure and diversity of a biofilm formed in a model drinking water distribution system. Appl. Env. Microbiol. 69 (11), 6899–6907.
Meissner, P.S., Falkinham, J.O., 1984. Plasmid-encoded mercuric reductase in Mycobacterium scrofulaceum. J. Bacteriol. 157 (2), 669.
Moritz, M.M., Flemming, H.-C., Wingender, J., 2010. Integration of Pseudomonas aeruginosa and Legionella pneumophila in drinking water biofilms grown on domestic plumbing materials. Int. J. Hyg. Env. Health 213 (3), 190–197.
Neu, L., Banziger, C., Proctor, C.R., Zhang, Y., Liu, W.-T., Hammes, F., 2018. Ugly ducklings-the dark side of plastic materials in contact with potable water. npj Biofilms Microbiomes 4.
Oliveira, I.M., Gomes, I.B., Simoes, L.C., Simoes, M., 2024. A review of research advances on disinfection strategies for biofilm control in drinking water distribution systems. Water Res. 253.
Pereira, A.C., Ramos, B., Reis, A.C., Cunha, M.V., 2020. Non-tuberculous mycobacteria: molecular and physiological bases of virulence and adaptation to ecological niches. Microorganisms 8 (9).
Pinto, M., Langer, T.M., Hueffer, T., Hofmann, T., Herndl, G.J., 2019. The composition of bacterial communities associated with plastic biofilms differs between different polymers and stages of biofilm succession. PLoS One 14 (6).
Pouey, J., Galey, C., Chesneau, J., Jones, G., Franques, N., Beaudeau, P., Mouly, D., Grp Referents Regionaux Ep, I, 2021. Implementation of a national waterborne disease outbreak surveillance system: overview and preliminary results, France, 2010 to 2019. Eurosurveillance 26 (34).
Proctor, C., Garner, E., Hamilton, K.A., Ashbolt, N.J., Caverly, L.J., Falkinham III, J.O., Haas, C.N., Prevost, M., Prevots, D.R., Pruden, A., Raskin, L., Stout, J., Haig, S.-J, 2022. Tenets of a holistic approach to drinking water-associated pathogen research, management, and communication. Water Res. 211.
Proctor, C.R., Dai, D., Edwards, M.A., Pruden, A., 2017. Interactive effects of temperature, organic carbon, and pipe material on microbiota composition and Legionella pneumophila in hot water plumbing systems. Microbiome 5 (1), 130.
Proctor, C.R., Reimann, M., Vriens, B., Hammes, F., 2018. Biofilms in shower hoses. Water Res. 131, 274–286.

Quast, C., Pruesse, E., Yilmaz, P., Gerken, J., Schweer, T., Yarza, P., Peplies, J., Glockner, F.O., 2013. The SILVA ribosomal RNA gene database project: improved data processing and web-based tools. Nucleic Acids Res. 41, 590–596.
R, J., George, Pine, W, M., Reeves, K., 1980. Amino acid requirements of Legionella pneumophila. J. Clin. Microbiol.
Ren, X., Han, Y., Zhao, H., Zhang, Z., Tsui, T.-H., Wang, Q., 2023. Elucidating the characteristic of leachates released from microplastics under different aging conditions: perspectives of dissolved organic carbon fingerprints and nano-plastics. Water Res. 233.
Rhoads, W.J., Ji, P., Pruden, A., Edwards, M.A., 2015. Water heater temperature set point and water use patterns influence Legionella pneumophila and associated microorganisms at the tap. Microbiome 3.
Rochex, A., Godon, J.-J., Bernet, N., Escudie, R., 2008. Role of shear stress on composition, diversity and dynamics of biofilm bacterial communities. Water Res. 42 (20), 4915–4922.
Romera-Castillo, C., Pinto, M., Langer, T.M., Alvarez-Salgado, X.A., Herndl, G.J., 2018. Dissolved organic carbon leaching from plastics stimulates microbial activity in the ocean. Nat. Commun. 9.
Samuelsson, J., Hallstrom, L.P., Marrone, G., Dias, J.G., 2023. Legionnaires' disease in the EU/EEA*: increasing trend from 2017 to 2019. Eurosurveillance 28 (11).
Sasada, R., Weinstein, M., Prem, A., Jin, M., Bhasin, J., 2020. FIGARO: an efficient and objective tool for optimizing microbiome rRNA gene trimming parameters. J. Biomol. Tech. 31 (Suppl), S2.
Schoen, M.E., Ashbolt, N.J., 2011. An in-premise model for Legionella exposure during showering events. Water Res. 45 (18), 5826–5836.
Shen, Y., Haig, S.-J., Prussin 2nd, A.J., LiPuma, J.J., Marr, L.C., Raskin, L., 2022. Shower water contributes viable nontuberculous mycobacteria to indoor air. PNAS Nexus 1 (5), 145-145.
Sheridan, E.A., Fonvielle, J.A., Cottingham, S., Zhang, Y., Dittmar, T., Aldridge, D.C., Tanentzap, A.J., 2022. Plastic pollution fosters more microbial growth in lakes than natural organic matter. Nat. Commun. 13 (1).
Shrout, J.D., Nerenberg, R., 2012. Monitoring bacterial twitter: does quorum sensing determine the behavior of water and wastewater treatment biofilms? Env. Sci. Technol. 46 (4), 1995–2005.
Soto-Giron, M.J., Rodriguez-R, L.M., Luo, C., Elk, M., Ryu, H., Hoelle, J., Domingo, J.W. S., Konstantinidis, K.T., 2016. Biofilms on hospital shower hoses: characterization and implications for nosocomial infections. Appl. Env. Microbiol. 82 (9), 2872–2883.
Stegen, J.C., Lin, X., Konopka, A.E., Fredrickson, J.K., 2012. Stochastic and deterministic assembly processes in subsurface microbial communities. ISME J. 6 (9), 1653–1664.
Taylor, M., Bentham, R.R., 2009. Legionella, protozoa, and biofilms: interactions within complex microbial systems. Microb. Ecol. 58 (3), 538–547.
Thomas, J.M., Thomas, T., Stuetz, R.M., Ashbolt, N.J., 2014. Your garden hose: a potential health risk due to Legionella spp. growth facilitated by free-living amoebae. Env. Sci. Technol. 48 (17), 10456–10464.
Waak, M.B., LaPara, T.M., Halle, C., Hozalski, R.M., 2018. Occurrence of Legionella spp. in water-main biofilms from two drinking water distribution systems. Env. Sci. Technol. 52 (14), 7630–7639.
Waak, M.B., LaPara, T.M., Halle, C., Hozalski, R.M., 2019. Nontuberculous mycobacteria in two drinking water distribution systems and the role of residual disinfection. Env. Sci. Technol. 53 (15), 8563–8573.
Wadowsky, R.M., Yee, R.B., 1983. Satellite growth of Legionella pneumophila with an environmental isolate of Flavobacterium breve. Appl. Environ. Microbiol. 46 (6), 1447–1449.
Wang, H., Masters, S., Hong, Y., Stallings, J., Falkinham III, J.O., Edwards, M.A., Pruden, A., 2012. Effect of disinfectant, water age, and pipe material on occurrence and persistence of Legionella, mycobacteria, Pseudomonas aeruginosa, and two amoebas. Env. Sci. Technol. 46 (21), 11566–11574.
Wang, H., Yu, P., Schwarz, C., Zhang, B., Huo, L., Shi, B., Alvarez, P.J.J., 2022. Phthalate esters released from plastics promote biofilm formation and chlorine resistance. Env. Sci. Technol. 56 (2), 1081–1090.
Wang, Y., Ogawa, M., Fukuda, K., Miyamoto, H., Taniguchi, H., 2013. Isolation and identification of mycobacteria from soils at an illegal dumping site and landfills in Japan. Microbiol. Immunol. 50 (7), 513–524.
Wen, G., Kötzsch, S., Vital, M., Egli, T., Ma, J., 2015. BioMig—a method to evaluate the potential release of compounds from and the formation of biofilms on polymeric materials in contact with drinking water. Env. Sci. Technol. 49 (19), 11659–11669.
Whiley, H., Giglio, S., Bentham, R., 2015. Opportunistic pathogens mycobacterium avium complex (MAC) and Legionella spp. colonise model shower. Pathogens 4 (3), 590–598.
Yang, X., He, Q., Liu, T., Zheng, F., Mei, H., Chen, M., Liu, G., Vymazal, J., Chen, Y., 2022. Impact of microplastics on the treatment performance of constructed wetlands: based on substrate characteristics and microbial activities. Water Res. 217.
Yao, M., Ren, A., Yang, X., Chen, L., Wang, X., van der Meer, W., van Loosdrecht, M.C.M., Liu, G., Pabst, M., 2024. Unveiling the influence of heating temperature on biofilm formation in shower hoses through multi-omics. Water Res. 268, 122704-122704.
Zhang, G., Li, B., Guo, F., Lin, J., Luan, M., Liu, Y., Guan, Y., 2019. Taxonomic relatedness and environmental pressure synergistically drive the primary succession of biofilm microbial communities in reclaimed wastewater distribution systems. Env. Int. 124, 25–37.
Zhao, E., Xiong, X., Li, X., Hu, H., Wu, C., 2024. Effect of biofilm forming on the migration of di(2-ethylhexyl)phthalate from PVC plastics. Env. Sci. Technol. 58 (14), 6326–6334.
Zhou, J., Ning, D., 2017. Stochastic Community Assembly: does it matter in microbial ecology? Microbiol. Mol. Biol. Rev. 81 (4). https://doi.org/10.1128/mmbr.00002-00017.